

## Structural studies of phosphorus induced dimers on Si(001)

Prasenjit Sen

*Harish-Chandra Research Institute  
Chhatnag Road, Jhansi, Allahabad 211019, INDIA.*

Bikash C. Gupta and Inder P. Batra

*University of Illinois at Chicago  
845 W. Taylor Street, Chicago Illinois 60607, USA.*

Renewed focus on the P-Si system due to its potential application in quantum computing and self-directed growth of molecular wires, has led us to study structural changes induced by P upon placement on Si(001)- $p(2 \times 1)$ . Using first-principles density functional theory (DFT) based pseudopotential method, we have performed calculations for P-Si(001) system, starting from an isolated P atom on the surface, and systematically increasing the coverage up to a full monolayer. An isolated P atom can favorably be placed on an **M** site between two atoms of adjacent Si dimers belonging to the same Si dimer row. But being incorporated in the surface is even more energetically beneficial due to the participation of the **M** site as a receptor for the ejected Si. Our calculations show that up to  $\frac{1}{8}$  monolayer coverage, hetero-dimer structure resulting from replacement of surface Si atoms with P is energetically favorable. Recently observed zig-zag features in STM are found to be consistent with this replacement process. As coverage increases, the hetero-dimers give way to P-P ortho-dimers on the Si dimer rows. This behavior is similar to that of Si-Si d-dimers but are to be contrasted with the Al-Al dimers, which are found between adjacent Si dimers rows and in a para-dimer arrangement. Unlike Al-Si system P-Si does not show any para to ortho transition. For both systems, the surface reconstruction is lifted at about one monolayer coverage. These calculations help us in understanding the experimental data obtained using scanning tunneling microscope.

PACS numbers: 68.43.Bc, 73.90.+f, 73.20.-r

### INTRODUCTION

Phosphorous-doped Si is the back-bone of micro-electronic technology. Recently, P-Si system has generated renewed interest due to its potential application in quantum computers [1, 2, 3] and growth of molecular wires on Si surfaces [4]. It is also of fundamental interest to compare the behavior of P-P dimers with Si-Si and Al-Al dimers on the Si surfaces, a lot having been understood about the last system [5, 6, 7].

Phosphine gas ( $\text{PH}_3$ ) is used as the source of P in most applications. Yu *et al.* [8] concluded from their experiments that around  $675^\circ\text{C}$ , all hydrogen atoms from  $\text{PH}_3$  are desorbed and the surface is a monolayer (ML) P covered Si(001) with the formation of P-P dimers. Wang *et al.* [9] did a scanning tunneling microscopy (STM) and Auger electron spectroscopy (AES) study of phosphorous-terminated Si(001) surface close to a monolayer P coverage. They find mostly P-P dimers, along with some Si-P dimers on the surface. They also find defects in the P-P dimer rows as well as anti-phase bound-

aries. At slightly below a ML P coverage, Wang *et al.* observe Si-Si, Si-P and P-P dimers. At still lower coverages, there are ‘significant’ numbers of Si-Si and Si-P dimers, while there are some P-P dimers. Kipp *et al.* [10] using STM, X-ray photoemission spectroscopy (XPS) and total energy calculations conclude that after low temperature  $\text{PH}_3$  adsorption there are dimers on the surface. It is not conclusive whether these are P-P, Si-P or Si-Si dimers, though they expect P-P dimers to be dominant at low temperatures. Both these groups (Wang *et al.* and Kipp *et al.*) observe similar ‘bright’ features above Si-Si surface dimers in their STM images at low P coverages. Wang *et al.* claim these to be indicative of Si-Si dimers, while Kipp *et al.* claim these to be P-P dimers. Curson *et al.* [11], from their STM studies, conclude that at low P coverages, the surface, in fact, contains Si-Si and Si-P dimers, thus supporting Wang *et al.*’s conclusions. Kipp *et al.* also found that after  $\text{PH}_3$  adsorption at  $625^\circ\text{C}$ , there are only symmetric P-P dimers on the surface. At the maximum P coverage, they find defects like missing dimer rows. From thermal desorption spectra of P

from the Si(001) surface, Hirose and Sakamoto [12] claim that at low coverages ( $< 0.2$  ML), there are mostly Si-P dimers on the surface. Above 0.2 ML coverage, P-P, Si-P dimers and defects coexist on the surface. Lin *et al.* [13] in their core-level photoemission and STM studies find that at  $\sim 700$  K the surface is interspersed with chains of P-P dimers. At  $\sim 800$  K the hydrogen atoms desorb completely and one observes partial replacement of Si atoms by P.

Thus apart from some differences in the details, most experiments agree that after the hydrogen from  $\text{PH}_3$  has been desorbed, the surface consists mostly of P-P dimers at higher coverages. At low coverages there is agreement that P replaces Si atoms and gets incorporated into the surface, but one would like to have a more detailed understanding of the structure.

There have been a few theoretical studies addressing the question whether  $\text{PH}_3$  adsorbs dissociatively or molecularly on Si(001) [14, 15, 16]. To our knowledge, there are no systematic theoretical studies of P-covered Si(001) surface as a function of coverage. Since it is the P atoms which are important in applications, one would like to understand their interaction with and structure on the Si(001) surface.

Therefore, we study stable atomic structure of P-covered Si(001) surface starting from a low coverage up to a ML. Apart from finding the most favorable binding site for a P ad-atom on this surface, we study P-P dimers on Si(001) in detail because they turn out to be a more favorable arrangement compared to isolated P atoms. We also compare the structure and energetics of P-P ad-dimers with Al-Al ad-dimers about which much is known. We arrive at the important conclusion that unlike Al-Si system, P-Si system always prefer an ortho-dimer structure and does not show a para to ortho transition with increasing coverage. Since P-Si hetero-dimers have been observed in experiments, we have also studied the energetics of replacement of surface Si atoms with P. In fact, at low P coverages, this replacement of surface Si atoms is a more favorable arrangement than adsorption of the P ad-atoms or dimers above the surface. Interestingly, the bright lines and zig-zag features observed in ref. [11] are related to this replacement process. In what follows, we discuss the methods used, and the results of our calculations in detail.

## METHOD

Calculations were performed using pseudopotential method within DFT. We use VASP [17, 18] for our calculations. The wave functions are expressed in a plane wave basis with an energy cutoff of 250 eV. The Brillouin zone integrations are performed using the Monkhorst-Pack scheme [19]. Ionic potentials are represented by ultrasoft Vanderbilt type pseudopotentials [20]. We use the generalized gradient approximation (GGA) [21] for the exchange-correlation energy. The preconditioned conjugate gradient method (as implemented in VASP) is used for wave function optimization and conjugate gradient is used for ionic relaxation. We use a  $(2 \times 2 \times 1)$   $\mathbf{k}$ -point mesh for our  $(4 \times 4)$  surface supercell, while for the  $(2 \times 2)$  surface supercell, we use a  $(4 \times 4 \times 1)$   $\mathbf{k}$ -point mesh. Convergence with respect to energy cutoff and number of  $\mathbf{k}$  points has been previously tested for similar systems [22, 23]. When making comparison between binding energies of structures with same supercell size, it is expected that the errors due to cutoff and  $\mathbf{k}$ -point mesh will cancel.

The Si(001) –  $p(2 \times 1)$  surface is represented by a repeated slab geometry. Each slab contains 5 Si atomic layers with hydrogen atoms passivating the Si atoms at the bottom layer of the slab. Consecutive slabs are isolated from each other by a vacuum space of 9 Å. The Si atoms in the top four atomic layers are allowed to relax, while the bottom layer Si atoms and passivating H atoms are kept fixed in order to simulate bulk-like termination. We reproduced the energetics and geometry of the  $p(2 \times 1)$  reconstructions of a clean Si(001) surface using the above parameters [24].

Our calculations provide cohesive energy of a supercell composed of given set of atoms,

$$E_C[SC] = E_T[SC] - E_A[atoms] \quad (1)$$

where  $E_C[SC]$  is the cohesive energy of the supercell,  $E_T[SC]$  is the total energy of the supercell, and  $E_A[atoms]$  is the total energy of all the isolated atoms that constitute the supercell. Thus  $E_C[SC]$  is the energy gained by assembling the given supercell structure from the isolated atoms. We define the binding energy (BE) of  $n$  P atoms,  $E_B$  as,

$$E_B = E_C[\text{Si}] - E_C[\text{Si} + n\text{P}] \quad (2)$$

where  $E_C[\text{Si}]$  is the cohesive energy of the Si slab, and  $E_C[\text{Si} + n\text{P}]$  is the cohesive energy with  $n$  P atoms ad-

sorbed/incorporated into the slab. The cohesive energies of the Si slab with and without P are calculated in the same supercell with fully relaxed atomic configurations. Written in terms of the total energies, it is easy to see from eqn. 1, that the BE can be expressed as,

$$E_B = E_T[\text{Si}] - E_T[\text{Si} + n\text{P}] + nE_A[\text{P}] \quad (3)$$

It should be noted that in order to compare stabilities of two structures, one should compare their formation energies (FE), which, in case of an ‘interstitial’ impurity (in this case, added P atoms may replace Si atoms in the slab, but they all remain within the system) can be written as [25]

$$E_{form} = E_T[\text{Si} + n\text{P}] - E_T[\text{Si}] - n\mu_P \quad (4)$$

where  $E_T[\text{Si} + n\text{P}]$  is the total energy of the Si slab with the  $n$  P atoms,  $E_T[\text{Si}]$  is the total energy of the Si slab, and  $\mu_P$  is the chemical potential of phosphorous in its reference state. In the case when different structures being compared have equal number of Si and P atoms, one can see from eqns 3 and 4 that comparing their FE’s is equivalent to comparing their BE’s, since difference in FE’s is just the negative of the difference in BE’s. Also, if the reference state is taken to be a gas of isolated atoms, which is probably appropriate in MBE conditions, then the FE of a structure is just the negative of its BE. However, in case of a ‘substitutional’ impurity, when a Si atom replaced by a P atom leaves the system and goes to a reservoir (again assumed to be a gas of isolated Si atoms), the formation energy is given by [25]

$$\begin{aligned} E_{form} &= E_T[(N - 1) \text{ atom Si slab} + \text{P}] \\ &- E_T[N \text{ atom Si slab}] \\ &+ E_A[\text{Si}] - E_A[\text{P}] \end{aligned}$$

Again, from eqn 1, it is easy to see that this is equal to the difference between the cohesive energies of an  $N$ -atom Si slab in which one Si is replaced by a P atom, and a the clean  $N$ -atom Si slab.

In this work, we mostly study stabilities of various structures having the same number of Si and P atoms, as suggested by experiments. Hence comparing their BE’s serves the purpose, higher BE implying a more stable structure. In case of an isolated P being incorporated in the Si slab, we also compare stabilities of these two structures: 1. the ejected Si remains in the slab; and 2. it goes to a reservoir. For this, we do have to compare the FE’s, as discussed in the next section.

## RESULTS AND DISCUSSIONS

In the subsequent subsections, we present results of our calculations in detail. We calculate the energetics of P adsorption on the surface, and replacement of surface Si atoms by P when we have an isolated P ad-atom, and at  $\frac{1}{8}$ ,  $\frac{1}{4}$ ,  $\frac{1}{2}$  and a full ML coverages.

### Isolated P ad-atom

As stated earlier, for P atoms on the Si(001) surface, we have considered two possibilities: they get adsorbed on the surface or they replace Si atoms and get incorporated into the surface. In the first case, we have calculated the BE of a single P ad-atom adsorbed at four symmetry sites on the  $p(2 \times 1)$  asymmetric Si(001) surface. The symmetry sites are: i) dimer site (**D**) on top of the Si surface dimer, ii) the site vertically above the second layer Si atom between two atoms of adjacent Si dimers belonging to the same dimer row (**M**), iii) cave site (**C**) between two Si surface dimers perpendicular to the dimer rows and iv) quasi-hexagonal site (**H**) half-way between two Si surface dimers along a dimer row. These sites are marked in fig 1. We used a  $(4 \times 4)$  surface supercell. The large size of the supercell ensures that the interaction between a P atom in our supercell and its periodic images are small and the BE represents that of an isolated P atom. While studying BE of a P ad-atom at these sites, we relax the P atom, and the top four Si layers. The BE values of the P atom at these sites are given in table I. In table I we also give BE of one P atom in a  $(2 \times 2)$  surface cell corresponding to  $\frac{1}{4}$  ML, which is discussed in detail later.

The **M** site turns out to be the most favorable site for an isolated P ad-atom. This is also the most favorable site for an isolated Si ad-atom on Si(001) first discovered by Brocks *et al.* [26]. Here P ad-atom binds to two Si atoms belonging to two different dimers in the same surface dimer row. These bonds are of equal length (2.3 Å) with Si-P-Si bond angle  $\sim 112^\circ$ , suggesting that P likes to be close to a tetrahedrally bonded configuration. Another significant observation is that the P ad-atom at the **M**-site is only 2.26 Å away from the second layer Si atom. This is a bond similar in character to the Si-P bonds at the surface as seen in the charge density plot in fig. 2(a). Thus the second layer Si atom bonded to P becomes five-fold coordinated probably accompanied by

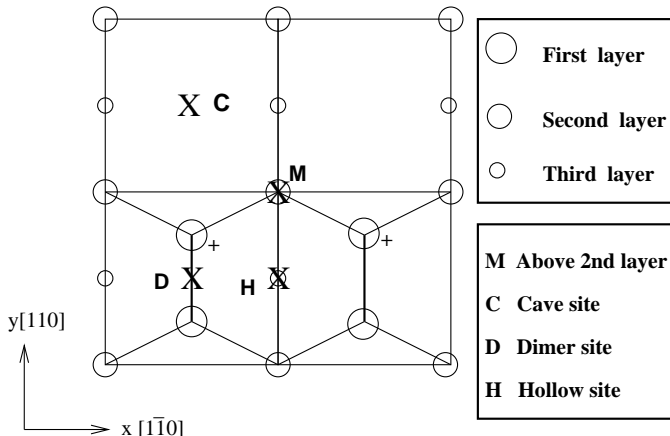


FIG. 1: Symmetry sites on the  $p(2 \times 1)$  asymmetric Si(001) surface at which binding properties of an isolated P ad-atom are studied. The Si atoms marked ‘+’ are at a greater height compared to their partners in the same dimer. This system size is for illustration only. Calculations have been done on different system sizes as discussed in the text.

weakening of its bonds with other Si atoms. This weakening of bonds costs energy, but P being 3-fold coordinated at the **M** site is beneficial energetically compared to the **D** site, where the P ad-atom is only two-fold coordinated. It is also found that when the P atom is at the **D** site, the Si-P-Si bonds make an angle of  $64^\circ$ . This angle is much smaller than an ideal tetrahedral angle of  $109^\circ$ . So there is a bond rotation on the P atom at the **D** site which costs energy. An interplay of these factors makes the **M** site more favorable by 0.2 eV compared to the **D** site. We show the charge density contour plots in the plane of the P ad-atom and the two surface Si atoms it binds with at the **M** and **D** sites in fig 2(b) and (c). The nature of P-Si bonding at the two sites is similar, so it is the bond rotation at the **D** site, and rearrangement of bonds the second layer Si atom forms, that make the **M** site more favorable.

Energetically, **M** and **D** sites are followed by the **H** and **C** sites. At the **H** and **C** sites, the P ad-atom can bind to four and two surface Si atoms respectively. However, being an *sp* element, and having a small atomic radius, it cannot take full advantage of all the neighboring surface Si atoms. Hence **H** site turns out to have a lower BE than the **M** and **D** sites. The **C** site has the lowest BE. It has been seen before that the size of an ad-atom

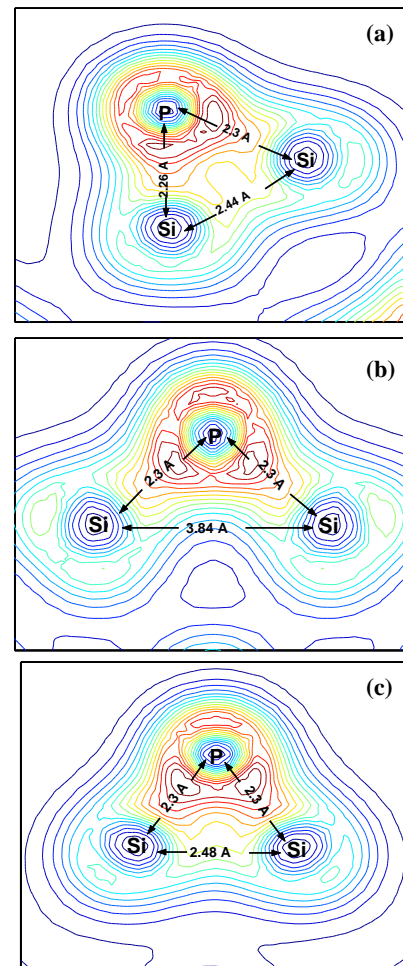


FIG. 2: (Color online) Charge density contour plots in the plane of the P ad-atom and the Si atoms it binds with. (a) P ad-atom at the **M** site bonded to a second layer Si atom and a surface Si atom; (b) P ad-atom at the **M** site bonded to two surface Si atoms of adjacent dimers in the same dimer row; (c) P ad-atom at the **D** site bonded to two Si atoms of the same surface dimer.

can have dramatic effects on its binding properties on a substrate [5]. Thus while the **M** site was found to be the most favorable site as stated before, for an Al ad-atom, **H** site turned out to be the most favorable [6, 26].

When the P atom gets incorporated into the surface we replace one of the Si atoms in a surface dimer on a  $(4 \times 4)$  cell by P. As for the ejected Si atom, it can either go to a reservoir, or bind with the Si surface at some other site. Experiments support the latter scenario [11, 16]. How-

TABLE I: BE (eV/atom) for an isolated P ad-atom at different symmetry sites on a Si(001)- $p(2 \times 1)$  surface at two different coverages.

| site     | isolated P | $\frac{1}{4}$ ML |
|----------|------------|------------------|
| <b>M</b> | 5.75       | 5.73             |
| <b>D</b> | 5.55       | 5.55             |
| <b>H</b> | 4.76       | 4.74             |
| <b>C</b> | 3.73       | 4.45             |

ever, for the sake of completeness, we have compared the energetics of these two scenarios, as discussed later. In cases where it remains in the system, we place the ejected Si atom at various sites on the surface. The possible initial geometries are shown in fig 3. Starting from these geometries, the ejected Si atom, top four atomic layers (including the incorporated P) are relaxed in all directions. It turns out that the energetically most favorable position for the ejected Si atom is geometry **I** marked in fig 3. This agrees with the results of Wilson *et al.* [16]. In the final relaxed geometry, the Si-P hetero-dimer moves by  $\approx 0.6$  Å along  $\langle \bar{1}\bar{1}0 \rangle$  compared to the Si-Si dimers on the clean surface. The adjacent Si-Si dimer, on the side of the ejected Si, moves by  $\approx 0.35$  Å along  $\langle \bar{1}\bar{1}0 \rangle$ . The two Si-Si dimers neighboring these two dimers also move by  $\approx 0.1$  Å along  $\langle \bar{1}\bar{1}0 \rangle$ . As noted, this movement of the dimers relative to the original surface dimers propagates along the dimer row up to at least 2 dimers away from the Si-P dimer (the maximum distance observable in a  $4 \times 4$  cell). The BE of the P atom in geometry geometry **I** is 6.1 eV. The BE's of the P atom in all the geometries studied are given in table II. Most importantly, comparing two situations with an isolated P atom on the surface: (i) when the P atom is adsorbed at the **M** site, and (ii) when it forms a P-Si heterodimer with the ejected Si in geometry **I**, the latter case is found to be more favorable by 0.4 eV. It is interesting to note that geometry **I** is reminiscent of Si ad-atom having **M** as the most favorable site [26]. The participation of **M** site makes Si replacement a favorable scenario. This is consistent with the observation that at low coverages, P atoms get incorporated into the Si surface.

We now ask whether it is more favorable for the ejected Si to remain in the system, or to go to a reservoir. For this, we compare the FE's of the following structures: 1. geometry **I** discussed above; 2. a P atom replacing a Si

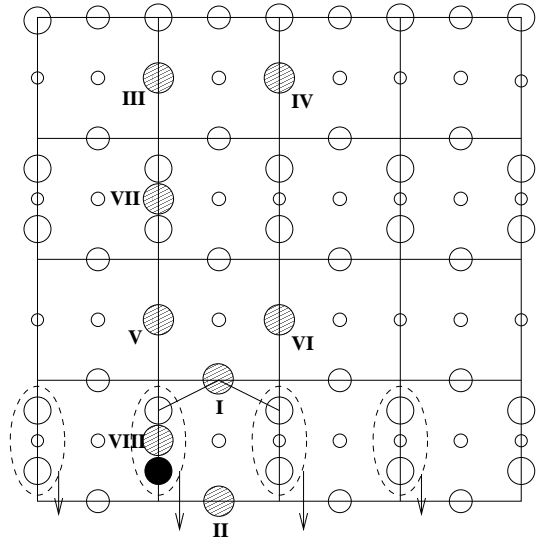


FIG. 3: Starting atomic geometries for studying incorporation of one P atom into a  $(4 \times 4)$  surface cell. The incorporated P atom is shown in dark color. Shaded circles show possible positions of the ejected Si atom, while open circles are the Si atoms in the slab. The movements of the Si-P dimer and Si-Si dimers neighboring it are indicated by the arrows.

atom in a surface dimer, and the ejected Si going to a reservoir that is assumed to be a gas of Si atoms. As argued in the METHOD section, the FE in the first case is just the negative of its BE, i.e.,  $-6.1$  eV. The FE in the second case, calculated as discussed in eqn. 5, turns out to be  $-1$  eV. Since higher FE means a less stable structure, clearly, it is more favorable for the ejected Si to remain within the system, a conclusion that matches with experimental observations. In all subsequent discussions, we assume that all the ejected Si atoms remain in the system.

### $\frac{1}{8}$ ML P Coverage

At a  $\frac{1}{8}$  ML coverage, again we consider two possibilities—P atoms replacing surface Si atoms, or they being adsorbed on the surface.

When the P atoms are adsorbed on the surface, we put 2 P ad-atoms on a  $(4 \times 4)$  surface supercell. Phosphorous being a pentavalent atom, even after binding to one or two surface Si atoms, we expect two P ad-atoms to dimerize if possible. This is borne out by our calcula-

TABLE II: BE in eV per P atom incorporated into the Si(001) surface with the ejected Si atom at different sites as discussed in the text.

| geometry    | BE  |
|-------------|-----|
| <b>I</b>    | 6.1 |
| <b>II</b>   | 5.2 |
| <b>III</b>  | 5.4 |
| <b>IV</b>   | 5.4 |
| <b>V</b>    | 4.9 |
| <b>VI</b>   | 5.2 |
| <b>VII</b>  | 5.4 |
| <b>VIII</b> | 5.1 |

tions at  $\frac{1}{4}$  ML, as we discuss later. Hence, at  $\frac{1}{8}$  ML, we consider possible positions of a P-P dimer. The *para*- and *ortho*-dimer arrangements are shown in fig. 4. We find that the ortho-dimer is a more favorable configuration of the P-P dimer, with a BE of 6.3 eV per P atom. The binding of the para-dimer turns out to be weaker with a BE of 5.9 eV per P atom.

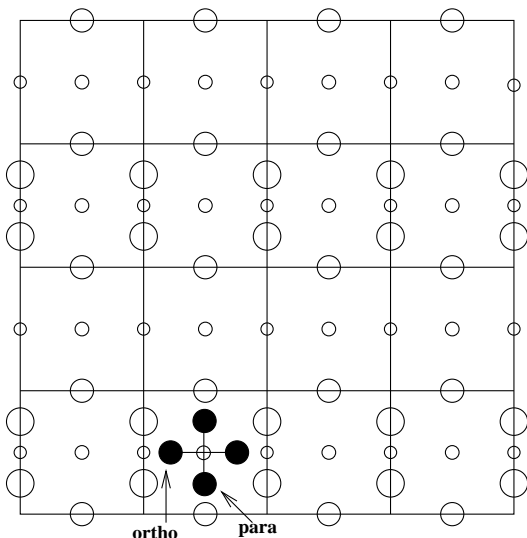


FIG. 4: The para- and ortho- orientations of a P-P dimer on the Si(001) surface at  $\frac{1}{8}$  ML studied in this work.

It is interesting to compare these energetics with those of Al-Al dimers on the Si(001) surface. The biggest difference between P-P and Al-Al dimers on Si(001) is that

while Al-Al dimers prefer to reside between surface dimer rows [6, 7], P-P dimers find it favorable to adsorb on top of dimer rows. We did study a P-P para-dimer in between two surface dimer rows, and the binding is found to be substantially weaker with a BE of 5.4 eV per P. Also, in the case of Al-Al dimers, at low coverages, the para-dimer configuration was found to be more favorable, while for P, ortho-dimer is more favorable. On the other hand, for a Si-Si ad-dimer on Si(001), Brocks *et al.* found that a para-dimer on a surface dimer row is only slightly more favorable by 0.1 eV compared to an ortho-dimer [5] (as this energy difference is the limit of the accuracy of their calculations). As we have found, a P ad-atom at the **M** site forms a bond with the second layer Si atom directly below it. This bond length is, in fact, slightly shorter than the bonds the P ad-atom makes with the surface Si atoms (see fig 2). This causes weakening of bonds between the second layer Si and other Si atoms, as we have already argued. One can view a para-dimer being formed by dimerization of two P ad-atoms on two **M** sites between two Si-Si dimers in the same surface dimer row. This stretches the P-second layer Si bonds, while the bonds between the second layer Si and other Si atoms are still weak. The overall effect is a net energy cost. In the ortho-dimer orientation, the P ad-atoms do not affect any second layer Si atoms, while they still dimerize and bind with four surface Si atoms. This situation turns out to be more favorable. In case of a Si ad-atom at the **M** site, the distance between the Si ad-atom and the second layer Si is found to be greater than bulk Si-Si distance, and also greater than the distance between the Si ad-atom and surface Si atoms [26]. Hence a Si ad-atom at the **M** site has negligible effect on the second layer Si atom. Thus even in a para-dimer orientation, there is not much energy cost in stretching the ad-atom-second layer bonds, and, in fact, para-dimer becomes more favorable for Si ad-dimers.

A side-view of the P-P ortho-dimer on the Si(001) surface is shown in fig 5. The P ad-atoms symmetrize the two adjacent Si-Si surface dimers, but do not break the dimers. Phosphorous atoms having smaller atomic radii than Si atoms, the P-P bond length is smaller ( $\sim 2.27$  Å). Hence the two adjacent Si-Si dimers are drawn in closer to the P-P dimer along  $\langle 1\bar{1}0 \rangle$  direction compared to their position on the  $p(2 \times 1)$ -asymmetric reconstructed surface. The Si-P distance in this case turns out to be  $\sim 2.3$  Å.

When two P atoms are incorporated, the ejected Si

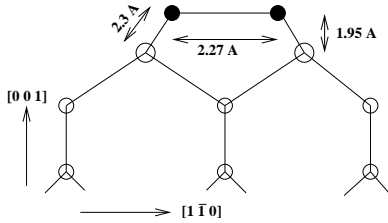


FIG. 5: Side-view of the local geometry around a P-P orthodimer adsorbed on Si(001). The P-P dimer is found to be symmetric.

atoms are placed at various sites on the surface and the geometries studied in this paper are shown in fig 6. Starting from these geometries, the ejected Si atoms, and top four atomic layers are relaxed. After relaxation, geome-

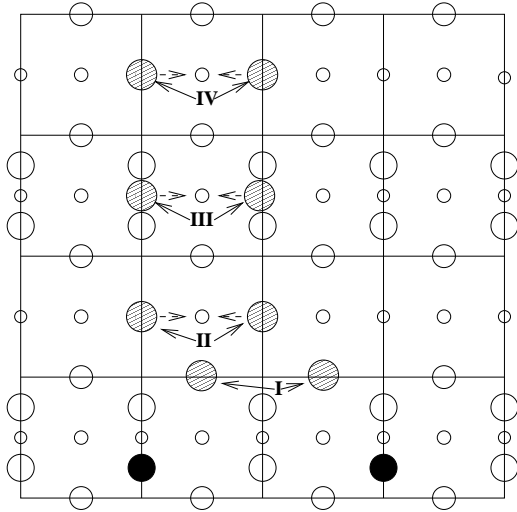


FIG. 6: Starting atomic arrangements for incorporation of two P atoms into  $(4 \times 4)$  surface cell. The P atoms are denoted by dark circles. Shaded circles show possible positions of the pair of Si atoms displaced by the P atoms. Small arrows indicate that the two ejected Si atoms form a dimer.

try **III** turns out to be the most favorable with a BE of 6.4 eV per P atom. Note that geometry **III** is an ortho-orientation of the Si-Si dimer on top of a surface dimer row. But it is known that the energy difference between the para- and ortho- configurations is small ( $\sim 0.1$  eV) [5], and hence either structure may be seen in experiments. In the final converged geometry, the two ejected Si atoms form an asymmetric dimer with a Si-Si distance of 2.39 Å.

In this geometry the dangling bonds of the four surface Si atoms, above which the ejected Si atoms dimerize, are saturated. The ejected Si atoms are also 3-fold coordinated. This large reduction of dangling bonds causes this geometry to be the most favorable. In geometry **I**, the next most favorable arrangement, the ejected Si atoms do not dimerize. In this geometry, four dangling bonds of the surface Si atoms are saturated, but the ejected Si atoms are only 2-fold coordinated. In geometries **II** and **IV** also, after relaxation, the ejected Si atoms form asymmetric dimers with Si-Si dimer distances of 2.38 Å and 2.41 Å respectively. However, in these two geometries, the surface Si atoms are quite far from the ejected Si's. Thus there is not much energy gain from bonding with surface Si atoms. This causes **II** and **IV** to be lower in BE. The BE's for all the geometries are given in table III.

TABLE III: BE per P atom for P incorporated into the Si(001) surface at  $\frac{1}{8}$  ML. The geometries refer to various positions of the ejected Si atoms as discussed in the text.

| geometry   | BE  |
|------------|-----|
| <b>I</b>   | 6.0 |
| <b>II</b>  | 5.6 |
| <b>III</b> | 6.4 |
| <b>IV</b>  | 5.7 |

Again, what is interesting to note is that the geometry with P atoms incorporated into the surface has a lower energy. Therefore, at low P coverages, it is more favorable for P atoms to replace surface Si atoms. The ejected Si atoms prefer to go in positions where the next layer of Si atoms would be above the starting surface, and form asymmetric dimers. This suggests that the bright lines seen in the STM images, along with the Si-P heterodimers are, in fact, ejected Si-Si dimers, and not P-P dimers. This is consistent with Curson *et al.*'s interpretation of the lines perpendicular to the surface dimer rows in their STM images as Si-Si dimer chains [11]. This also supports Wang *et al.*'s interpretation of their STM images [9].

Curson *et al.* have observed some zig-zag features in their STM images [11]. There is also a bright spot associated with this feature as seen in those images. There could be two possible origins of these, (i) P-Si heterodimer, which, as already mentioned, move by 0.6 Å rel-

ative to the Si-Si dimers, or (ii) the ejected Si atom in geometry **I** in fig. 3. Charge density contours in a horizontal plane approximately  $\sim 1 \text{ \AA}$  above the Si-P dimer (without the ejected Si atom at **I**) are shown in fig. 7. A zig-zag feature is distinctly visible. There is also an excess charge density on the P atom in the displaced dimer which can appear as a bright spot in STM. In a charge density plot (not shown here) on a similar plane  $\sim 1 \text{ \AA}$  above the ejected Si in geometry **I**, only the Si atom is seen and no zig-zag features, since the surface dimer rows are not visible any more. From these observations we conclude that the zig-zag features and the associated bright spots can be attributed to Si-P hetero-dimers.

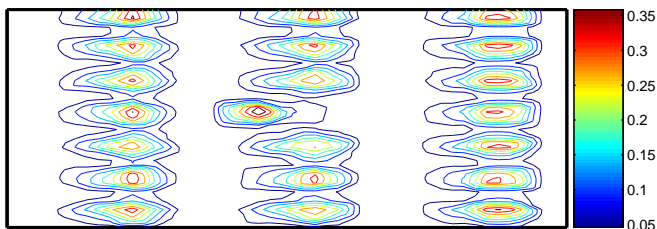


FIG. 7: (Color online) Charge density contour plots in a plane  $\sim 1 \text{ \AA}$  above the Si-P dimer. The displacement of the Si-P dimer gives it a zig-zag appearance in STM. Larger charge on the P atom is also visible. This can give rise to the associated bright spot.

#### $\frac{1}{4}$ ML P coverage

At  $\frac{1}{4}$  ML P coverage also we study both the possibilities—P getting adsorbed on the surface, or getting incorporated into the surface. For each of these possibilities, we do calculations on two different system sizes—(i) one P atom on a  $(2 \times 2)$  surface cell, (ii) four P atoms on a  $(4 \times 4)$  surface cell.

When we have four P ad-atoms adsorbed on a  $(4 \times 4)$  cell, they would form two P-P ortho-dimers. Various reasonable positions of two P-P dimers are shown in fig 8. The BE's for the relaxed structures starting from these atomic configurations are given in table IV. The dimers prefer to be separated by at least two lattice spacings (of the square lattice on the unreconstructed Si(001) surface) along the  $\langle 110 \rangle$  direction. In fact, there is essentially no difference in energy between structures **II** and **III**. This shows that there is no further energy gain in moving the

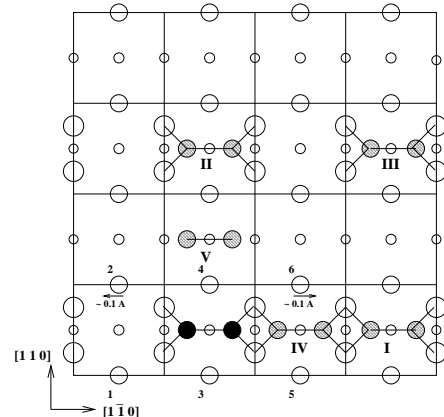


FIG. 8: Initial geometries for two P-P dimers on a  $(4 \times 4)$  supercell studied in this work. Given one dimer in a position indicated by the dark circles, five possible positions are shown for the second dimer. Movements of two second layer Si atoms (marked **2** and **6**) when only the dark dimer is present on the surface are also shown.

second dimer along  $\langle 1\bar{1}0 \rangle$  once we have moved it along  $\langle 110 \rangle$  by two lattice spacings. On the other hand, putting two dimers only one lattice spacing apart, either along  $\langle 110 \rangle$  or  $\langle 1\bar{1}0 \rangle$  costs energy. Thus structures **IV** and **V** are less favorable than **II** or **III**, **IV** being costlier than **V**.

In order to understand why structures **II** and **III** turn out be lower in energy than **I**, one has to look at the structure around the P-P dimer more closely. As we have already mentioned, top layer Si-Si dimers neighboring a P-P dimer are drawn closer to it. On the other hand, there are six second layer Si atoms (marked **1-6** in fig 8) immediately neighboring a P-P dimer (marked by dark circles in that figure). Of these, two second layer atoms (**2** and **6**) actually move away from the P-P dimer, while the others remain in their ideal positions as on a bare surface. When two P-P dimers are put in structure **I**, the second layer Si in between them (**6** in this case) is frustrated since the two dimers tend to push it in opposite directions. This causes strain in the structure. There is no such problem once the P dimers are separated by at least two lattice spacings along  $\langle 110 \rangle$ , in which case all second layer Si atoms neighboring the P dimers can relax freely. The fact that structures **II** and **III** have the same energy also indicates that this relaxation of the second layer Si atoms is a crucial mechanism in optimizing the structure. Once that has been achieved in structure **II**,



there is no further energy gain in moving the second P dimer two lattice spacings along  $\langle 1\bar{1}0 \rangle$ .

TABLE IV: BE values in eV per P atom for two P-P dimers present on a  $(4 \times 4)$  surface supercell of Si(001) starting from various initial atomic geometries as discussed in the text.

| geometry   | BE  |
|------------|-----|
| <b>I</b>   | 6.2 |
| <b>II</b>  | 6.3 |
| <b>III</b> | 6.3 |
| <b>IV</b>  | 5.7 |
| <b>V</b>   | 5.8 |

In structures **IV** and **V**, two P dimers are put one lattice spacing apart in the initial configuration. Atomic relaxation starting from these geometries indicate that it is energetically highly unfavorable for two P-P dimers to come so close to each other at this coverage. There is a repulsion between the two dimers and they tend to move away from each other.

Now we present our results for  $\frac{1}{4}$  ML P coverage studied with one P ad-atom on a  $(2 \times 2)$  surface supercell. We put the P ad-atom at **M**, **D**, **H**, and **C** sites. A look at table I shows that BE's at **M**, **D** and **H** sites are essentially the same as those for an isolated Si atom. However, binding at the **C** site is significantly stronger in the present case. At **M**, **D** and **H** sites, an isolated P atom is already reasonably strongly bonded to the neighboring surface Si atoms. However, the P-Si bonding at the **C** site is rather weak, which leaves the isolated P ad-atom with localized electrons on it. At  $\frac{1}{4}$  ML, the P atom finds other P atoms at nearby **C** sites, which gives these localized electrons a channel to delocalize. This delocalization lowers the kinetic energy of the electrons, and makes the binding stronger. We also find that at  $\frac{1}{4}$  ML coverage, two P-P dimers on a  $(4 \times 4)$  surface cell have a stronger binding than a single P ad-atom on a  $(2 \times 2)$  surface cell. This shows that dimer formation by P ad-atoms on the Si(001) surface significantly lowers their energy.

In case of P incorporation into the surface, when we have one P atom on a  $(2 \times 2)$  surface cell, the ejected Si is placed in geometry **I** as explained in fig 3. The ejected Si and top four atomic layers are relaxed. In the converged geometry, the BE is found to be 6.1 eV per

P ad-atom. While putting four P atoms on a  $(4 \times 4)$  surface cell, there can be several possibilities. However, we are guided by our calculations at  $\frac{1}{8}$  ML, where we found that two ejected Si atoms prefer to dimerize on top of and perpendicular to surface Si dimer row. We thus incorporated all the four P atoms in the dimers in a row of our  $(4 \times 4)$  cell, and put the ejected Si atoms above the other dimer row. The starting configuration is shown in fig 9. In the relaxed geometry, the ejected Si atoms form two asymmetric dimers, as expected. The BE turns out to be 6.2 eV per P atom. There is slight energy gain relative to the  $(2 \times 2)$  cell due to dimerization of ejected Si atoms.

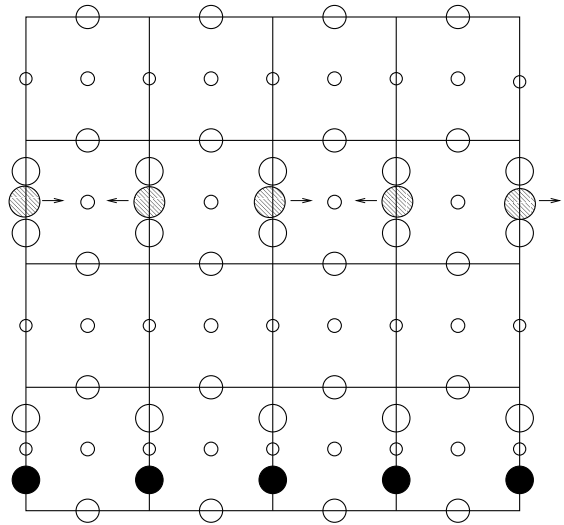


FIG. 9: Starting geometry for the four ejected Si atoms (shaded circles) when four P atoms (dark circles) are incorporated in a  $(4 \times 4)$  surface cell.

Now a comparison of BE's for P adsorbed and P incorporated geometries shows that at  $\frac{1}{4}$  ML, P adsorption is more favorable than P incorporation by 0.1 eV. Thus we reach the significant conclusion that at a critical coverage whose value lies between  $\frac{1}{8}$  ML and  $\frac{1}{4}$  ML, P atoms prefer to get adsorbed on the surface and form P-P orthodimers, rather than getting incorporated in the surface. Note that, while at  $\frac{1}{4}$  ML P adsorption is more favorable, in experiments, it is not surprising to find some P incorporation concurrently.

### $\frac{1}{2}$ and full ML P coverage

At  $\frac{1}{2}$  ML also we calculated the energetics of P incorporation into Si(001) surface, though it is expected that adsorption would be more favorable at this coverage. In fact, that is what we find in our calculations. In order to study adsorption at  $\frac{1}{2}$  ML P coverage, we put two P ad-atoms in a dimerized position on a  $(2 \times 2)$  surface cell. We again calculated energies of P-P para-dimer and ortho-dimer on top of a surface dimer row. These two geometries are shown in fig. 10(a). It turns out that the ortho-dimer is a more favorable configuration. The P-P dimer distance is found to be  $2.27 \text{ \AA}$  while the Si-P distance is  $2.34 \text{ \AA}$ . The underlying Si dimers are symmetrized, but the Si-Si dimer distance still remains to be  $2.33 \text{ \AA}$ . Thus the local geometry and bonding around a P-P ad-dimer is similar to that found around an ad-dimer in case of  $\frac{1}{8}$  ML with a similar value for the BE. The BE turns out to be  $6.3 \text{ eV}$  per P atom. The para-dimer configuration has a BE of  $5.9 \text{ eV}$  per P. So we find another crucial difference between Al-Al and P-P dimers on Si(001). Al-Al dimers showed a transition from a para- to ortho- orientation with increasing coverage [7], but P-P dimers always prefer an ortho- orientation.

In order to study P incorporation, we replace two Si atoms in two dimers on a  $(2 \times 2)$  surface cell by P atoms. There are several possibilities where the ejected Si atoms can go. We have considered four possible arrangements for two ejected Si atoms that are shown in Fig. 10(b). The geometry **I** and the ortho-dimer geometry (**III**) of the Si atoms turn out to be very close in BE. The BE of geometry **III** is  $5.97 \text{ eV}$  per P atom and that of geometry **I** is  $5.95 \text{ eV}$  per P atom. The para-dimer geometry (**IV**) has a BE of  $5.45 \text{ eV}$  per P atom. Geometry **II** turns out to be the least favorable with a BE of  $5.12 \text{ eV}$  per P atom.

At one ML coverage, we put four P atoms on a  $(2 \times 2)$  surface supercell. Again, a symmetric dimer-row structure of the P ad-atoms turns out to be the most favorable one. This is same as the structure found for a ML As-covered Si(001). The geometry of a full ML P covered Si(001) is shown in fig. 11. The P-P dimer distance in the the relaxed structure is calculated to be  $2.3 \text{ \AA}$ . The Si-P distance is found to be  $2.38 \text{ \AA}$ . The BE for P-P ad-dimers is found to be  $6.4 \text{ eV}$  per P atom at full ML coverage. Another important feature seen at this coverage is that the reconstruction of the underlying Si surface is lifted, just as was found for As on Si(001). We have seen that

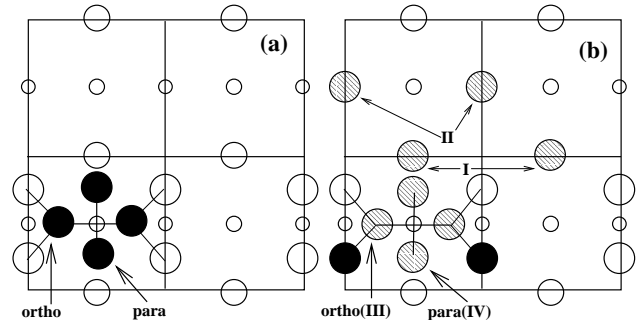


FIG. 10: Two P atoms (dark circles) on a  $(2 \times 2)$  surface cell at half monolayer coverage. (a) Para- and ortho-dimer configurations of two adsorbed P-P dimer; (b) two P atoms replace two surface Si atoms (shaded circles), which are shown in four different initial geometries.

it is unfavorable for two P-P dimers to come too close to each other on the surface. Some of this strain could be released by missing P-P dimer rows as found in experiments. However, since we are studying full ML coverage with a  $(2 \times 2)$  surface supercell, we cannot explore this possibility in our calculations.

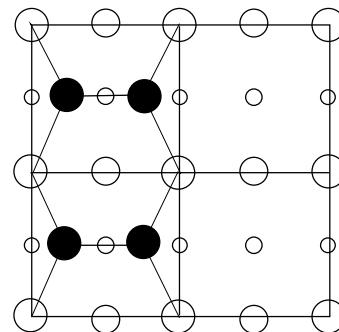


FIG. 11: Four P ad-atoms (dark circles) forming two dimers on a  $(2 \times 2)$  surface cell at a full ML coverage. Reconstruction of the underlying Si(001) surface is lifted.

Our findings that at higher coverages P adsorption becomes more favorable, and that P ad-atoms prefer to form dimers, are consistent with the conclusions reached by Yu *et al.* and Wang *et al.* [8, 9].

## CONCLUSIONS

We have done a systematic first-principles pseudopotential density functional study of structural changes induced by P on Si(001). For adsorption of an isolated P atom, the **M** site turns out to be energetically most favorable. However, up to a P coverage of  $\frac{1}{8}$  ML, replacement of surface Si atom by P is even more beneficial energetically due to the participation of the **M** site. The resulting Si-P hetero dimers give rise to the zig-zag and associated bright features in STM images. The ejected Si atoms prefer to form dimer chains perpendicular to the surface dimer rows. At some critical coverage between  $\frac{1}{8}$  ML and  $\frac{1}{4}$  ML, adsorption of P becomes more favorable than incorporation into the surface. At all coverages, P-P ortho-dimers on top of Si dimer rows are more favorable than para-dimers. This is in contrast to Al-Al dimers on Si(001) which prefer to reside between surface dimer rows, and show a transition from an para- to ortho-orientation with increasing coverage. At  $\frac{1}{2}$  ML coverage P ad-atoms also form dimers. At a full ML coverage P atoms show a propensity to form dimer rows after lifting reconstruction of the Si surface. There could be some missing dimer rows to relieve strain in the system.

- 
- [1] J. L. O'Brien, S. R. Schofield, M. Y. Simmons, R. G. Clark, A. S. Dzurak, N. J. Curson, B. E. Kane, N. S. McAlpine, M. E. Hawley, and G. W. Brown, *Phys. Rev. B* **64**, 161401 (2001).
- [2] S. R. Schofield, N. J. Curson, M. Y. Simmons, F. J. Ruess, T. Hallam, L. Oberbeck, and R. G. Clark, *Phys. Rev. Lett.* **91**, 136104 (2003).
- [3] B. E. Kane, *Nature (London)* **393**, 133 (1998).
- [4] Y. Wang and G. S. Hwang, *App. Phys. Lett.* **86**, 023108 (2005).
- [5] G. Brocks, P. J. Kelly, and R. Car, *Surf. Sc.* **269/270**, 860 (1992).
- [6] G. Brocks, P. J. Kelly, and R. Car, *Phys. Rev. Lett.* **70**, 2786 (1993).
- [7] B. C. Gupta and I. P. Batra, *Phys. Rev. B* **69**, 165322 (2004). Also see I. P. Batra, *Phys. Rev. Lett.* **63**, 1704 (1989).
- [8] M. L. Yu, D. J. Vitkavage, and B. S. Meyerson, *J. Appl. Phys.* **59**, 4032 (1986).
- [9] Y. Wang, M. J. Bronikowski, and R. J. Hamers, *Jl. Phys. Chem.* **98**, 5966 (1994); Y. Wang, X. Chen, and R. J. Hamers, *Phys. Rev. B* **50**, 4534 (1994); J. Shan, Y. Wang, and R. J. Hamers, *Jl. Phys. Chem.* **100**, 4961 (1996).
- [10] L. Kipp, R. D. Bringans, D. K. Biegelsen, J. E. Northrup, A. Garcia, and L.-E. Swartz, *Phys. Rev. B* **52**, 5843 (1995).
- [11] N. J. Curson, S. R. Schofield, M. Y. Simmons, L. Oberbeck, J. L. O'Brien, and R. G. Clark, *Phys. Rev. B* **69**, 195303 (2004).
- [12] R. Hirose and H. Sakamoto, *Surf. Sc.* **430**, L540 (1999).
- [13] D.-S. Lin T.-S. Ku, and T.-J. Sheu, *Surf. Sc.* **424**, 7 (1999); D.-S. Lin T.-S. Ku, and R.-P. Chen, *Phys. Rev. B* **61**, 2799 (2000).
- [14] R. Miotto, G. P. Srivastava, and A. C. Ferraz, *Phys. Rev. B* **63**, 125321 (2001).
- [15] P.-L. Cao, L.-Q. Quan, J.-J. Dai, and R.-H. Zhou, *Jl. Phys.: Cond. Mat.* **6**, 6103 (1994).
- [16] H. F. Wilson, O. Warschkow, N. A. Marks, S. R. Schofield, N. J. Curson, P. V. Smith, M. W. Randy, D. R. McKenzie, and M. Y. Simmons, *Phys. Rev. Lett.* **93**, 226102 (2004).
- [17] G. Kresse and J. Furthmüller, *Phys. Rev. B* **54**, 11 169 (1996).
- [18] G. Kresse and J. Hafner, *Phys. Rev. B* **47**, R558 (1993).
- [19] H. J. Monkhorst and J. D. Pack, *Phys. Rev. B* **13**, 5188 (1976).
- [20] D. Vanderbilt, *Phys. Rev. B* **41**, 7892 (1990); G. Kresse and J. Hafner, *Jl. Phys.: Cond. Mat.* **6**, 8245 (1994).
- [21] J. P. Perdew and Y. Wang, *Phys. Rev. B* **46**, 6671 (1992).
- [22] P. Sen, S. Ciraci, I. P. Batra, and C. H. Grein, *Phys. Rev. B* **64**, 193310 (2001).
- [23] A. J. Ciani, P. Sen, and I. P. Batra, **69**, 245308 (2004).
- [24] A. Ramstad, G. Brocks, and P. J. Kelly, *Phys. Rev. B* **51**, 14 504 (1995).
- [25] G. M. Dalpian, Antônio J. R. da Silva, and A. Fazzio, *Phys. Rev. B* **68**, 113310 (2003).
- [26] G. Brocks, P. J. Kelly, and R. Car, *Phys. Rev. Lett.* **66**, 1729 (1991).